EUROPEAN SYNCHROTRON RADIATION FACILITY

INSTALLATION EUROPEENNE DE RAYONNEMENT SYNCHROTRON

# Experiment Report Form

| | | |
|---|---|---|
| | **Experiment title:**<br>**Quantification of COVID-19's Impact on Lung Structure: from Whole Lobe to Alveolar Capillary Scales** | **Experiment number**:<br>MD1252 |
| **Beamline**: | **Date of experiment**:<br>from: 14 May 2020 to: 27 July, 2021 | **Date of report**:<br>06/01/22 |
| **Shifts:** | **Local contact(s)**:<br>Paul Tafforeau, Elodie Boller | *Received at ESRF:* |


**Names and affiliations of applicants** (* indicates experimentalists):

Prof. Peter D Lee (Department of Mechanical Engineering, University College London)

Dr. Paul Tafforeau (ESRF)

Dr. Claire Walsh, Joseph Brunet, Patrick Xian (UCL)

Dr. Elodie Boller (ESRF)

Med. Dr. Wagner Willi (Laboratory Heidelberg University Diagnostic and Interventional Radiology)

Prof. Dr. Danny Jonigk, PD Dr. Christopher Werlein, PD Dr. Mark Kuehnel (Hannover Medical School)


**Report: Final**


**Abstract:**

Imaging intact human organs from the organ to the cellular scale in three dimensions is a goal of biomedical imaging. To meet this challenge, we developed hierarchical phase-contrast tomography (HiP-CT), an X-ray phase propagation technique using the European Synchrotron Radiation Facility (ESRF)'s Extremely Brilliant Source (EBS). The spatial coherence of the ESRF-EBS combined with our beamline equipment, sample preparation and scanning developments enabled us to perform non-destructive, three-dimensional (3D) scans with hierarchically increasing resolution at any location in whole human organs. We applied HiP-CT to image five intact human organ types: brain, lung, heart, kidney and spleen. HiP-CT provided a structural overview of each whole organ followed by multiple higher-resolution volumes of interest, capturing organotypic functional units and certain individual specialized cells within intact human organs. We demonstrate the potential applications of HiP-CT through quantification and morphometry of glomeruli in an intact human kidney and identification of regional changes in the tissue architecture in a lung from a deceased donor with coronavirus disease 2019 (COVID-19).


**Specific developments of BM05 include**

- Specimen preparation – development of an ethanol/ethanol agarose mounting procedure to prevent motion and bubbling;

- Sample holders - 8 environmental precision sample holders were produced and shipped to ESRF to enable micron precision repositioning of samples in separate containers (allowing the physicians to pick the zoom regions before remounting); these remain with ESRF;
- Reconstruction algorithm - significant changes in the reconstruction to remove low frequency background effects; and image normalisation (to remove vertical gradients in flux);
- Image segmentation - machine learning and various quantification of the resulting structures in the highly damaged and heterogeneous COVID-19 damaged lungs, have been expanded upon;
- All resulting in the development of the Hierarchical Phase-Contrast Tomography technique, HiP-CT, published in Nature Methods[1].

All of these advances have enabled:

1. Quantification of the spatial heterogeneity of COVID-19 damage across donor lungs. This was achieved via quantifying airspace morphology changes. Parameters captured.
2. *3D assessment of COVID-19 lung's anatomic distribution of vascular and parenchymal abnormality*.
3. Characterisation of clinical CT features such as "tree and bud", which are visible in COVID-19 pneumonia medical CT, but not understood.
4. Collected over 52 human organs from both control (LADAF) and COVID Hannover donors
5. Detailed hierarchical imaging over 35 organs both COVID-19 and Control have been performed.
6. Scans of lung biopsy pathologies performed ~ 65
7. Visual inspection of all biospies scan performed by expert radiologist and histopathologist for abnormalities and data curation. Specific scans selected for analysis of fibrosis patterns.
8. 1 publication in Nature Methods Altimeric score of 1993 and 58K accesses. [1]
9. 1 Publication (Ackermann et al.) in the Blue Journal where HiP-CT was used to identify anastmosis between the pulmonary and bronchiole vascular supplies in the lungs of COVID-19 donors. [2]
10. 1 pre-print of a data paper detailing the anatomy of the control human lung at multiple scales.
11. Half a dozen papers in preparation.
12. Histology of organs after HiP-CT scanning reveals no obvious structural damage and proves equivalence of resolution for highest resolution HiP-CT and histology.
13. A publicly available database of the lungs, heart, brain, kidney, spleen has been created and published www.human-organ-atlas.esrf.eu . There have been over 716 downloads of the raw data. This is set to be expanded to include COVID-19 organs and become a gold standard atlas of organs that is at least two orders of magnitude higher resolution than prior databases (e.g. the Visible Human Project, www.nlm.nih.gov/research/visible/visible_human.html)

**Methods:**

Lungs, brain, heart, kidney and liver were collected from COVID-19 patients during autopsies in Hannover, or from Autopsy performed at the LADAF. Samples were embalmed and then immersion fixed for over 72h in 4% formalin and transferred to 70% ethanol (using stepped increase from 50-70% to minimise shrinkage and damage), leaving no viable tissue, cells or organisms (see Fig. 1A for full method). Organs were sent to ESRF where they were stabilised in an agar-agar gel and degassed before mounting in jars and Double walled precision environmental chambers were designed and manufactured (see figure 1C) to hold the fixed whole lobe samples (ca. 100x100x300mm) and enable them to be taken on/off the beamline.

The HiP-CT scanning procedure adapts two protocols originally developed to image large fossils. The first, the attenuation protocol, normalizes absorption in the field of view[3,4]; whereas the second, the accumulation protocol, provides extended dynamic range[5]. At 25 μm per voxel, HiP-CT scans are dominated by attenuation; hence, there is reduced contrast sensitivity and a requirement for more accumulations, whereas higher resolutions are dominated by phase, leading to fewer accumulations. The dominance of attenuation at lower resolution creates horizontal line artifacts during concatenation of radiographs due to the vertical profile of the beam. To remove these artifacts, the vertical profile residual background after flat-field correction is subtracted before reconstruction. For higher-resolution scans in which phase effects dominate, this step is not required.

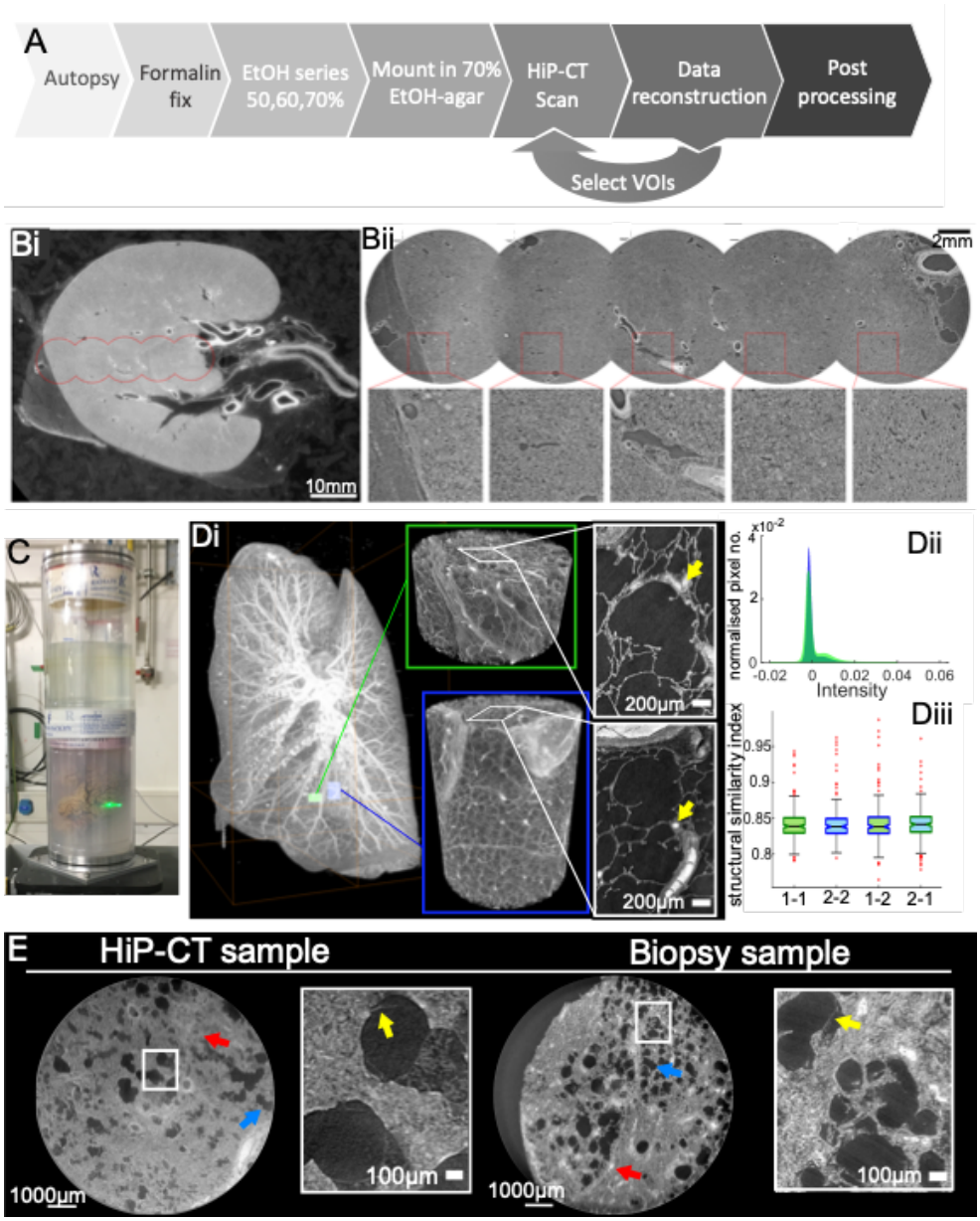


*Figure 1:* ***a****, Flow chart of HiP-CT sample preparation and imaging procedure; the ability to select specific higher-resolution scan regions based on lower-resolution scans provides hierarchical tissue structure images in a data-efficient manner.* ***b****, Left, 2D image slice (25 μm per voxel) showing the location of a series of regions of 2.5 μm per voxel that transect the organ's radius (red circles). Right, HiP-CT scans at 2.5 μm per voxel every 7 mm from the external kidney surface (left) to the centre of the sample (right). Scans are overlapped and stitched to provide a complete organ. The magnified view shows a constant level of data quality and precision over the complete transect through the use of the reference scan procedure.* ***c****, Photograph of an intact human brain mounted in a polyethylene terephthalate jar with ethanol–agar stabilization and with the reference jar on top.* ***d****, Left, maximum intensity projection of a whole human lung with two randomly selected VOI imaged at a resolution of 2.45 μm per voxel shown in green (VOI1) and blue (VOI2). Three-dimensional reconstructions of the two high-resolution VOI are shown with 2D slices in the insets. In the 3D high-resolution VOI, the fine mesh of pulmonary blood vessels and the complex network of pulmonary alveoli and their septa can be seen. Yellow arrows denote occluded capillaries in 2D slices. Top right, image stack histograms for the green (VOI1) and blue (VOI2) high-resolution VOI, respectively (fixed bin width, 0.0001). Intensity distributions are comparable with positive skew (1.82 and 2.68) and kurtosis (6.44 and 11.88) for VOI1 and VOI2, respectively; the histogram intersection is 71 ± 3% for fixed bin width in the range $1 \times 10^{-2} - 3 \times 10^{-4}$. Bottom right, box-and-whisker plot showing the structural similarity index between n = 200 pairs of 2D slices independently sampled either from within the same VOI (1-1 and 2-2) or from different VOI (1-2 and 2-1) for each group, respectively; one-way ANOVA (two sided); P = 0.8765, three degrees of freedom, F = 0.23). Box plots show the median (centre line), interquartile range (75th–25th percentiles) of data (box bounds) and data range excluding outliers (whiskers)); values more than 1.5 times the interquartile range above or below box bounds are denoted as outliers (red crosses).* ***e****, Single representative slices of high-resolution scans from a HiP-CT image of an intact whole human lung lobe affected by COVID-19 (donor 3) and a biopsy taken from the same patient's contralateral lung. Both VOI are captured from the upper peripheral region of each upper lung lobe. In HiP-CT images, fine structure of the tissue including blood capillaries (red arrows) and alveoli (blue arrows) as well as thin alveolar septa (yellow arrows in insets) is depicted.*

HiP-CT scans are performed hierarchically, the first typically at 25 µm per voxel over the whole organ followed by VOI at 6.5 µm per voxel and 1.3–2.5 µm per voxel. Scanning time for HiP-CT is faster than that for other techniques[6,7] , currently ~16 h for a whole brain at 25 µm per voxel and ~3.5 h for a whole kidney at 25 µm per voxel. The experimental setup is largely automated and can be adjusted to increase scanning speed for smaller organs while accommodating different fields of view for higher-resolution imaging. Our scanning procedure allows users to select high-resolution VOI with the spatial context provided by the preceding lower-resolution scans

Lung biopsy samples were also prepared and scanned to compare to HiP-CT (Fig 1E).

**Results:**

*Technique development:*
After preprocessing of radiographs to generate high-quality local tomography, image reconstruction can be performed using a filtered back-projection algorithm, coupled with single-distance phase retrieval[8], combined with a two-dimensional (2D) unsharp mask performed on the projection phase maps as implemented in PyHST2 software[9]. All subscans (covering typically 2.5 mm vertically) are concatenated after reconstruction. Subsequently, residual ring artifacts that would not have been removed in the preceding steps are corrected on reconstructed slices[10].
Using this pipeline we estimated the resolution of HiP-CT by Fourier shell correlation (FSC) analysis[11,12]. Resolution was estimated at the half-bit criterion to be 10.4 µm ± 0.17 µm for images at 2.5 µm per voxel, 18.3 µm ± 0.6 µm for images at 6.5 µm per voxel and 72 µm ± 3.4 µm for images at 25 µm per voxel. To assess the consistency in the quality of higher-resolution scans at different tissue depths and distances from the rotational centre of the intact organ, we analysed intensity distributions across two high-resolution VOI. We found that the image intensity histograms had an intersection of 71% ± 3%. Both distributions showed positive skewing and kurtosis with minimal differences in mean intensities between the different VOI (Fig. 1d, top right). In addition, we quantified differences in image quality between the two volumes using the structural similarity index[13] (Fig. 1c and Fig. 1d, bottom right). No significant difference in structural similarity index (median values, 0.839–0.841, $P = 0.88$) was observed across compared image volumes, indicating that HiP-CT can achieve high-resolution scanning in any region of the intact human lung with consistent quality.
We also qualitatively compared high-magnification HiP-CT scans of an intact human lung and a physically subsampled biopsy (cylindrical biopsy, 8.1 mm in diameter, 14 mm in height). The image quality of the two samples was found to be indistinguishable (Fig. 1e). The fine structure of the lung tissue including capillaries and alveoli was depicted in a histopathologically correct and undistorted manner, with very thin membranes within the alveoli (yellow arrows) being some of the smallest structures (thickness of ~5 µm) evident in both samples.

By performing histopathological analysis following HiP-CT on areas of the organs that have received the highest X-ray dose we have demonstrated that HiP-CT does not cause observable morphological damage, leaving the tissue available for subsequent analysis not limited to histology but potentially also to spatial transcriptomics. Histological comparison also facilitates and validates our interpretations/segmentations of HiP-CT, a key factor in developing image processing pipelines (Figure 1).

*Mapping human organs*
We applied HiP-CT to image multiple length scales in a variety of human organs. Intact lung, heart, kidney, spleen and brain (Figure 2). At 25 µm per voxel, macroscopic features of each organ were unambiguously identifiable through anatomical location and morphology including sulci and gyri of the cerebral cortex (Fig. 2a(i,ii)), individual lobules of the lung (Fig. 2b(i,ii)), the four chambers of the heart and associated coronary arteries (Fig. 2c(i,ii)), the pelvis and calyces of the kidney (Fig. 2d(i,ii) ) and the pulpa of the spleen (Fig. 2e(i,ii)).
In the brain, layers of the cerebellum were visible (Fig. 2a(iii,iv)), and a number of individual Purkinje cells were evident between the molecular and granule cell layers, identifiable by their distinctive pyramidal cell body and anatomical location[14] (Fig. 2a(iv,v)). In the lung, the intralobular septa and septal veins were visible (Fig. 2b(iii)) along with the terminal bronchi, which lead into acini. Within the acini, cup-shaped alveoli, across which gas exchange occurs, brightly contrasted cell-sized objects mainly at intersections of alveolar septa, were evident, which we identified as type II pneumocytes and/or alveolar macrophages based on comparative

histology (Fig. 2b(iv,v)). Bundles of cardiac muscle fibres were visible in the heart (Fig. 2c(iii)), consisting of individual cardiomyocytes, which could be distinguished by their distinctive shape and arrangement in fascicles and by comparative histology[15] (Fig. 2c(iv,v)). In the kidney, epithelial tubules comprising the nephron were evident (Fig. 2d(iii)), which, at their apex, harboured the intricate capillary network of the glomerulus (Fig. 2d(iv,v)), specialized for filtration of blood. Finally, the organization of red and white pulp in the spleen (Fig. 2e(iii)) was visible, the former containing splenic sinuses and the latter containing periarterial lymphoid sheaths and lymphocyte-rich follicles (Fig. 2e(iv,v)). Collectively, these images show that HiP-CT is capable of imaging intact human organs down to the resolution of organotypic functional units and certain types of specialized cells.

To exemplify how HiP-CT may be used in organ-wide mapping of tissue functional units, we have performed image segmentation and analysis on the smallest functional unit of the kidney – the glomerulus; measuring the total number, distribution and morphology of glomeruli across the kidney. These compare well to established histology methods and provide new measures such as surface area that cannot be measured with existing techniques.

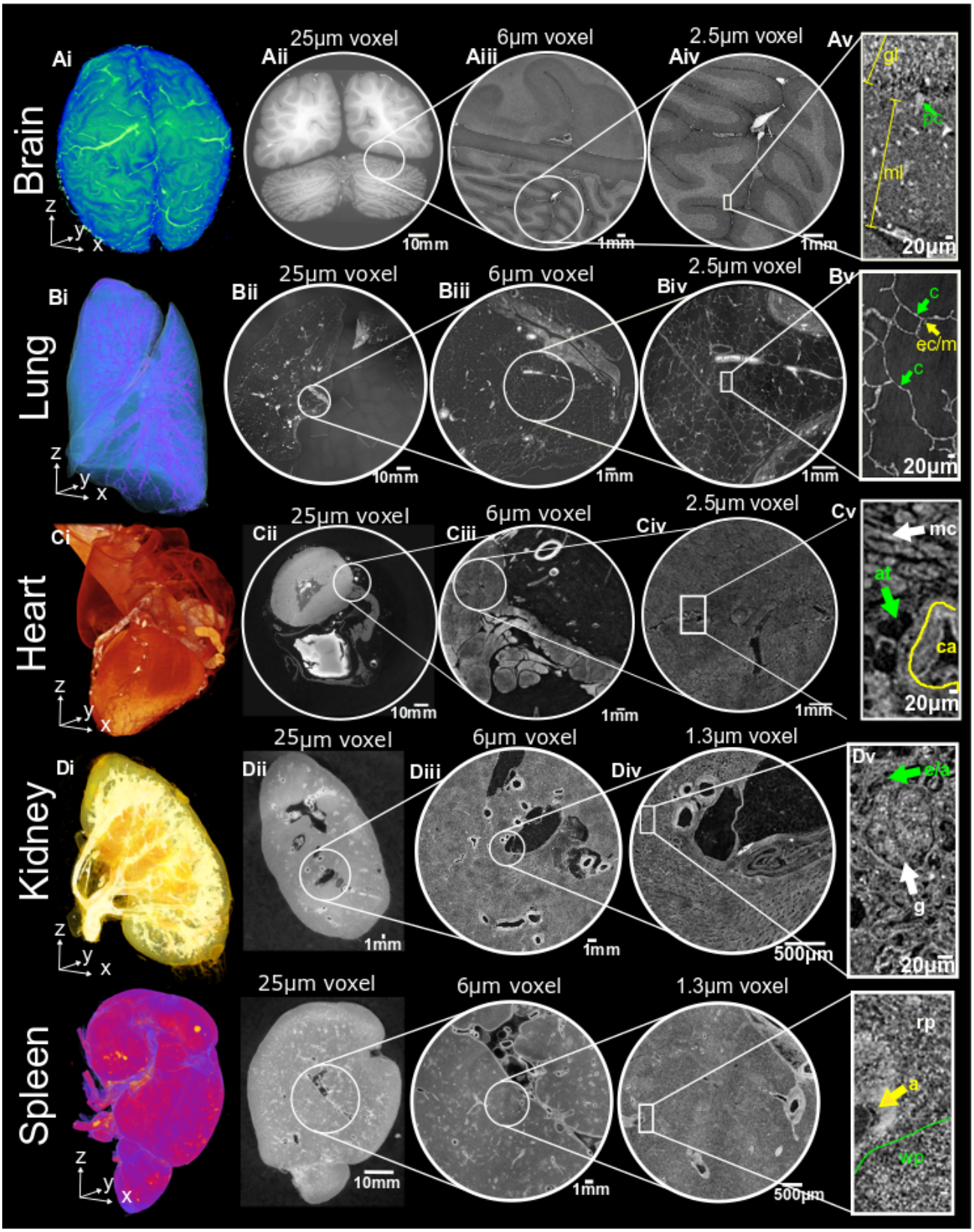


*Figure 2: HiP-CT has redefined the resolution at which organs can be imaged, and an **"atlas of organs"** will be available from the ESRF website of the organotypic structural and functional units of whole human organs. For each organ A) brain, B) lung, C) heart, D) kidney, E) spleen, panel (i) shows a 3D rendering of the whole organ from scans at 25µm. Subsequent 2D slices (ii-iv) show the higher resolution scan area marked on its preceding scan. (v) shows a digital zoom of the highest resolution image and in each case the arrows depict a characteristic structural feature of the respective organ. Av) molecular layer (ml), granular layer (gl), purkinje cell (pc). Bv) capillary (c), epithelial cell/macrophage (ec/m); Cv) myocardium (mc), coronary artery (ca), adipose tissue (at). Dv) efferent/afferent arteriole (e/a),glomerulus (g). Ev) red pulp (rp), white pulp (wp), arteriole (a).*

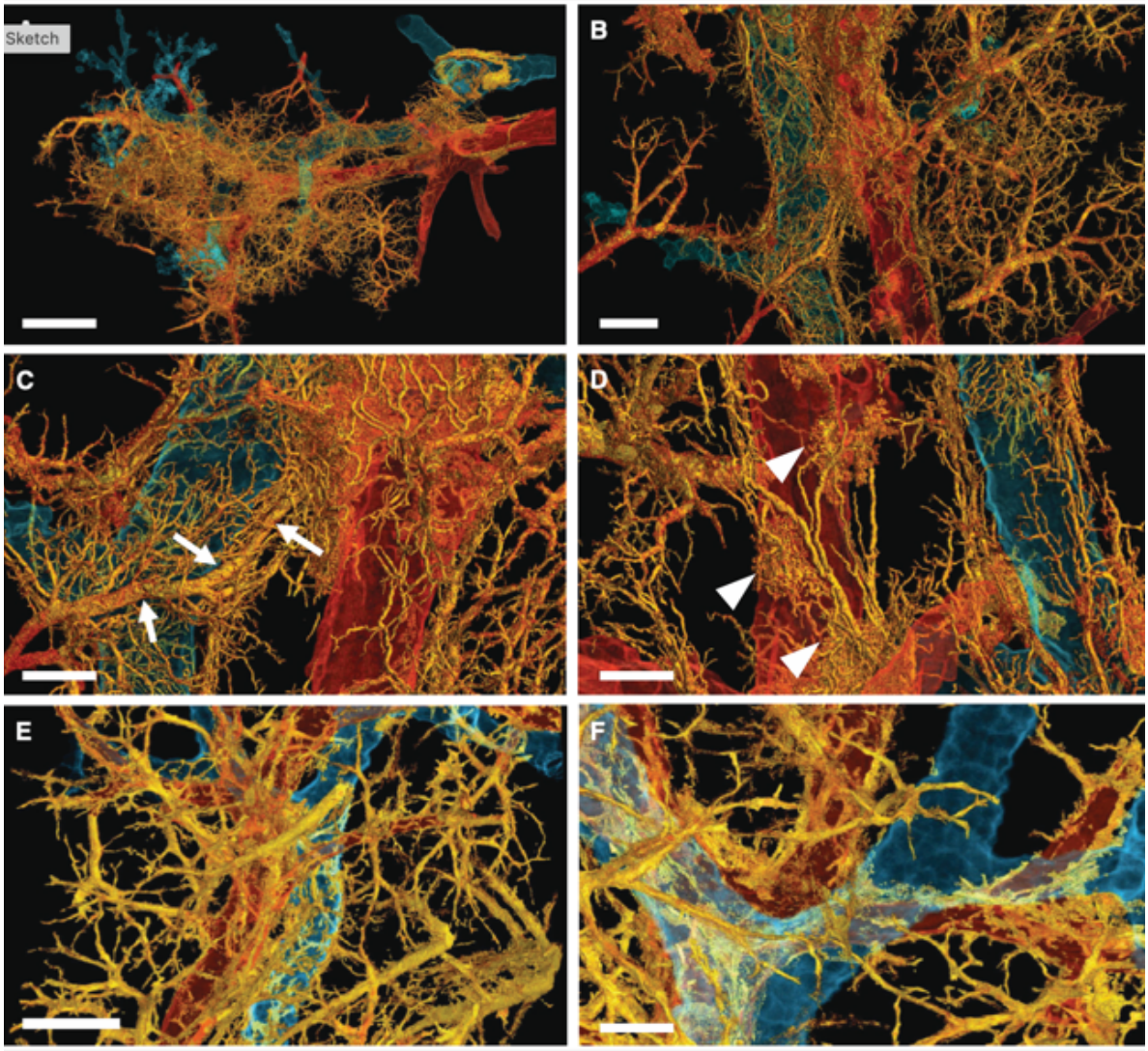


*Figure 3. Three-dimensional complexity of vascular remodeling and bronchiopulmonary shunting in coronavirus disease (COVID-19) highlighted by hierarchical phase-contrast tomography. (A) The distal bronchiole (blue) is paralleled by a centrilobular pulmonary artery (red) and an expanded plexus of private vessels (vasa vasorum) (yellow) in a secondary pulmonary lobule in the periphery of the left lower lobe. Scale bar, 4 mm. (B) Dilatation and expansion of the peribronchiolar plexus and vasa vasorum (yellow) is observed around the distal terminal bronchiole (blue) and centrilobular pulmonary artery (red). Scale bar, 1.3 mm. (C) Numerous arteriovenous anastomoses (yellow) form between bronchial arteries and pulmonary artery drain into a pulmonary vein accompanied by a pronounced shunting of a Sperrarterie (white arrows). These specialized arteries are essential for intrapulmonary arteriovenous shunting and are located mainly at the septal margin of secondary pulmonary lobules, where up to 3 to 5 such "Sperrarterien" anastomoses can be found in each lobule. Scale bar, 0.7 mm. (D) The perivascular vasa vasorum and bronchial vascular plexus are characterized by complex nodular lesions with angiomatoid- and plexiform-like arrangements (white arrowheads). Scale bar, 0.7 mm. For high-resolution details, see COVID-19 Pneumonia in the online supplement . (E) In controls, the vascular architecture shows a well-organized hierarchy of peribronchial vessels. Scale bar, 1.3 mm. (F) Only few perivascular vasa vasorum are observed in healthy control tissue. Scale bar, 0.7 mm. For high-resolution details, see Control in the online supplement.*

*COVID-19 analysis*

Imaging the COVID-19 lung across various length scales in 3D has enabled clinicians to explore the extent and type of COVID-19 damage. In doing so several new hypotheses concerning the pathogenesis of COVID-19 have been confirmed such as the anastomosis of pulmonary and bronchiole vascular systems Figure 3 (2). A spatial analysis of peribronchial vessels in COVID-19 pneumonia by hierarchical phase-contrast tomography demonstrated the expansion of peribronchial and perivascular arteriovenous anastomoses and a recruitment of "Sperrarterien" (blockade arteries) across individual secondary pulmonary lobules in the third dimension for the first time (Figures 3A and 3B). This intralobular shunting is accompanied by different spots of glomerouid-like vascular expansion (Figures 3C and 3D).

We have also published quantitative analysis of the structural changes in the airspace morphology of in the COVID-19 lung as compared to a healthy control lung. We have shown that alveoli septum thickness increases, there is an overall loss of patent alveoli and alveoli ducts are dilated. We have shown significant differences in these damage patterns both within a single COVID-19 lung and as compared to a control lung. (Further details in [1]).

In addition to these published findings, we have also performed analyses demonstrating a co-localistation of specific damage patterns with secondary pulmonary lobule boundaries (conference presentation pending). HiP-CT data has been combined with clinical radiology datasets of COVID-19 where it has provided the means to correlate microstructural features to new phenomenon seen in clinical data e.g. airway tree-and-bud structures (publication in preparation). As well as to provide correlation and to molecular data to understand how molecular changes in patterns of angiogenesis lead to structural changes across the areas of the lung (publication in preparation).

**Conclusions:**

Through our various methodological developments, we have develop a new overarching methodology, HiP-CT, that enabled hierarchical 3D imaging of multiple intact human organs, providing consistently high imaging quality from whole human organs down to individual organotypic functional units and certain specialized cells at any location within the organ.

Our exemplar of multiscale glomerular analysis demonstrates the benefit of hierarchical imaging with representative subsampling to estimate the number and morphology of spatially disparate (glomerular) organotypic features. We also leveraged the advantages of HiP-CT for multiscale and quantitative 3D analyses in pathological contexts, identifying and quantifying regional changes in the architecture of the air–tissue interface and alveolar morphology in the lung of a donor with confirmed pulmonary COVID-19 disease.

HiP-CT has considerable translational potential for biomedical applications, which we demonstrated by 3D imaging of a SARS-CoV-2-infected lung. In addition to reproducing the histopathological hallmarks of COVID-19, HiP-CT revealed extensive regional heterogeneity in parenchymal damage, and arteriovenous anastomosis. Our HiP-CT approach clearly demonstrates how physical subsampling methods that aim to infer organ-wide pathophysiology could be confounded by such heterogeneity. This potential confounder is surmounted by HiP-CT due to its flexibility in the scale of tissue volume that can be imaged, independent of location and over a wide range of resolutions. Moreover, quantitative analysis of lung architecture from HiP-CT images aligns with clinicopathological observations of an increased volume of ventilated air that does not participate in gas exchange in COVID-19-related ARDS[16]. Further HiP-CT investigation of COVID-19-related ARDS requires refinement using image-analysis methodologies such as machine learning. HiP-CT could also be used to provide insights into the secondary consequences of COVID-19 in other organs, such as the kidney and brain, both of which show evidence of tropism for SARS-CoV-2.

**Future work**

HiP-CT will evolve alongside advances in synchrotron technology. Here, we present results using our experimental method developed on a test beamline (BM05). The completion of a new beamline at the ESRF, BM18, in 2022 is anticipated to provide increased resolution in volumes several times larger than human organs while using lower doses of X-rays with improved sensitivity and a much higher speed. Such fourth-generation synchrotron sources may herald new possibilities in the life sciences.BM18, specifically for phase imaging of large samples will dramatically increase the capabilities of this technique by making it possible to perform HiP-CT on the complete human body scale, with zooming capabilities down to the histological level, at lower X-ray doses.

## References


1. Walsh, C.L., Tafforeau, P., Wagner, W.L. *et al.* Imaging intact human organs with local resolution of cellular structures using hierarchical phase-contrast tomography. *Nat Methods* **18,** 1532–1541 (2021). https://doi.org/10.1038/s41592-021-01317-x
2. Ackermann M, et al. The Bronchial Circulation in COVID-19 Pneumonia. Am J Respir Crit Care Med. 2022 Jan 1;205(1):121-125. doi: 10.1164/rccm.202103-0594IM. PMID: 34734553.
3. Carlson, K. J. et al. The endocast of MH1, *Australopithecus sediba*. *Science* **333**, 1402–1407 (2011).
4. Sanchez, S., Fernandez, V., Pierce, S. E. & Tafforeau, P. Homogenization of sample absorption for the imaging of large and dense fossils with synchrotron microtomography. *Nat. Protoc.* **8**, 1708–1717 (2013).
5. Voeten, D. F. A. E. et al. Wing bone geometry reveals active flight in *Archaeopteryx*. *Nat. Commun.* **9**, 923 (2018).
6. Zhao, S. et al. Cellular and molecular probing of intact human organs. *Cell* **180**, 796–812 (2020).
7. Edlow, B. L. et al. 7 Tesla MRI of the ex vivo human brain at 100 micron resolution. *Sci. Data* **6**, 244 (2019).
8. Paganin, D., Mayo, S. C., Gureyev, T. E., Miller, P. R. & Wilkins, S. W. Simultaneous phase and amplitude extraction from a single defocused image of a homogeneous object. *J. Microsc.* **206**, 33–40 (2002).
9. Mirone, A., Brun, E., Gouillart, E., Tafforeau, P. & Kieffer, J. The PyHST2 hybrid distributed code for high speed tomographic reconstruction with iterative reconstruction and a priori knowledge capabilities. *Nucl. Instrum. Methods Phys. Res. B***324**, 41–48 (2014).
10. Lyckegaard, A., Johnson, G. & Tafforeau, P. Correction of ring artifacts in X-ray tomographic images. *Int. J. Tomogr. Stat.* **18**, 1–9 (2011).
11. Krenkel, M. et al. Phase-contrast zoom tomography reveals precise locations of macrophages in mouse lungs. *Sci. Rep.* **5**, 9973 (2015).
12. Salditt, T. & Töpperwien, M. Holographic imaging and tomography of biological cells and tissues. In *Nanoscale Photonic Imaging* (eds Salditt, T., Egner, A. & Luke, D. R.) **134**, 339–376 (Springer, 2020).
13. Wang, Z., Bovik, A. C., Sheikh, H. R. & Simoncelli, E. P. Image quality assessment: from error visibility to structural similarity. *IEEE Trans. Image Process.* **13**, 600–612 (2004).
14. Kahle, W. & Frotscher, M. *Color Atlas and Textbook of Human Anatomy. Nervous System and Sensory Organs* (Thieme, 1986).
15. Iaizzo, P. A. (ed.) *Handbook of Cardiac Anatomy, Physiology, and Devices*. (Springer, 2009).
16. Grasselli, G. et al. Pathophysiology of COVID-19-associated acute respiratory distress syndrome: a multicentre prospective observational study. *Lancet Respir. Med.* **8**, 1201–1208 (2020).


## Impact

The results of this work are contributing towards 5 manuscripts to date, and over a dozen talks presented. A joint feasibility award to UCL, ESRF, Hannover and Mainz from the Chan Zuckerberg Initiative has been made to demonstrate the feasibility of imaging tissue at a cellular level in deep in large organisms including the human body. This has provided 2 PhD studentships and 2.5 yrs funding for 3 Research Fellows. It was recently extended to make BM18 usable for this project faster and more efficiently, providing funding to ESRF to further develop and placing UCL staff at ESRF.

## Manuscripts resulting and under preparation from MD1252 beam time:

| **Title** | **Imaging intact human organs with local resolution of cellular structures using hierarchical phase-contrast tomography** |
|---|---|
| Authors | C. L. Walsh, P. Tafforeau, W. L. Wagner, D. J. Jafree, A. Bellier, C. Werlein, M. P. Kühnel, E. Boller, S. Walker-Samuel, J. L. Robertus, D. A. Long, J. Jacob, S. Marussi, E. Brown, N. Holroyd, D. D. Jonigk, M. Ackermann and P. D. Lee |
| Link | https://www.nature.com/articles/s41592-021-01317-x |
| **Title** | **The bronchial circulation in Covid-19 pneumonia** |
| Authors | M. Ackermann, P. Tafforeau, W. L. Wagner, C. L, Walsh, C. Werlein, M. P. Kühnel, F. P. Länger, C. Disney, A. J. Bodey, A. Bellier, S. E. Verleden, P. D. Lee, S. J. Mentzer and D. D. Jonigk<br>Journal: American Thoracic Society |
| Link | https://www.atsjournals.org/doi/abs/10.1164/rccm.202103-0594IM |

| Title | **A multiscale X-ray phase-contrast tomography dataset of whole human left lung** |
|---|---|
| Authors | R. P. Xian, C. L. Walsh, S. E. Verleden, W. L. Wagner, A. Bellier, S. Marussi, M. Ackermann, D. D. Jonigk, J. Jacob, P. D. Lee, and P. Tafforeau |
| Link for pre-print | https://www.biorxiv.org/content/10.1101/2021.11.20.469361v1 |

## Publications under preparation

1. Wagner, Tafforeau et al, "Vascular Tree-in-bud in COVID-19 assessed by Hierarchical Phase-Contrast Tomography and correlative Histopathology", in preparation.
2. Ackermann et al. "Evidence of endothelial-mesenchymal transition in early fibrotic remodeling of COVID-19 patients" in preparation.
3. Jafree and Walsh et al. "Mapping human nephron density and morphology with Hierarchical Phase-Contrast Tomography", in preparation.
4. Walsh, Ramani and Jafree, et al. "COVID-19 impact on kidney vascular geometry" in preparation.
5. Ramani et al. "The Human renal vascular network" in preparation.
6. Brunet et al. "Sample preparation and stabilization for high-resolution synchrotron x-ray tomographic imaging of intact human organs " in preparation.
7. Brunet, Xian, Walsh et al. "Operando monitoring of X-ray-induced bubble formation in wet soft tissue imaging" in preparation.

## Further funding:

| Funder | Proposal Title |
|---|---|
| MRC | Imaging Dynamics In Biophysical/biochemical Processes Across The Hierarchical Scales (BioPro Network) |
| MRC | BioGrOA: Imaging Joint Biomechanics In Growth And Osteoarthritis |
| CZI | HiP-CT Imaging Hub |
| CZI | Deep Tissue Imaging RFA Feasibility Grant: Anatomical to Cellular Synchrotron Imaging of the Whole Human Body |
| EPSRC | Tomo-SAXS: Imaging full-field molecular-to-macroscale biophysics of fibrous tissues |
| EPSRC | Assessing Placental Structure and Function by Unified Fluid Mechanical Modelling and in-vivo MRI |
| EPSRC | Oncological Engineering - A new concept in the treatment of bone metastases |

## Plenary, Keynote, Invited and other talks at International Conferences and Workshops

10 presentations

1. P D Lee, "The Human Organ Project using the ESRF-EBS", **Invited**, Institute of Healthcare Engineering Colloquium.
2. C Walsh, "The Human Organ Project: Multiscale synchrotron imaging of whole organs to single

cells without sectioning" at Developmental Biology and Cancer programme meeting UCL-Institute for Child Health.

3. PD Lee, “Seeing Materials Through a Synchrotron Looking Glass: Inside Additive Manufacturing to Intact Covid-19 Injured Organs with Micron Resolution” **Inaugural lecture**, Danish Lighthouse Initiative, Nov. 6, 2021
4. PD Lee, “Orthogonal and complementary approaches panel”, 2021 HCA General Meeting
5. C Walsh et al, "Hierarchical Phase-Contrast Tomography imaging of multi-scale structural lung damage across in COVID-19”, **Invited**, ESRF User meeting 2021.
6. D D Jonigk and M Ackermann, "COVID19 - 3D imaging for deciphering the pathology of a global pandemic", **Keynote**, ESRF user meeting 2021.
7. J Jacob, "COVID Imaging Studies at UCL and UCLH", **Invited,** at UCLH BRC Covid Research Seminar.
8. C Walsh, "Multi-scale imaging and analysis of intact human organs with Hierarchical Phase contrast tomography, (HiP-CT)", **Invited,** Hard X-ray Imaging of Biological Soft Tissues Symposium.
9. P D Lee, "The Human Organ Atlas in Health and Disease. Created using Hierarchical Phase-Contrast Tomography (HiP-CT).", **Invited,** Chan Zuckerberg Science Initiative 5-Year Anniversary Symposium.
10. P Tafforeau “From fossils to human organs, development of synchrotron phase-contrast hierachical imaging at the ESRF” **Keynote**, Helmholtz Imaging Conference 2021

YouTube channel (HiP-CT, 365 subscribers, 55,326 views) and Twitter (@hip_ct) reach.